Polymer Journal (2019) 51:869–882
https://doi.org/10.1038/s41428-019-0208-1

ORIGINAL ARTICLE

The inherent blue luminescence from oligomeric siloxanes

Yuqun Du[1,2] · Tian Bai[1,2] · Fan Ding[1,2] · Hongxia Yan[1,2] · Yan Zhao[1,2] · Weixu Feng[1,2]

Received: 2 January 2019 / Revised: 5 May 2019 / Accepted: 7 May 2019 / Published online: 28 May 2019

Abstract

Luminescent polymers without traditional aromatic groups have attracted great attention due to their excellent biocompatibility and promising applications. Understanding of the luminescence mechanism of such polymers, however, is still in its infancy. To further reveal the fluorescence mechanism in depth, two kinds of oligomeric siloxanes were skillfully elaborated and fabricated via a convenient and facile one-pot transesterification polycondensation reaction under catalyst-free conditions. Intriguingly, oligomeric siloxanes bearing nonconventional chromophores show bright blue fluorescence under 365 nm UV lamp illumination. Our preliminary results demonstrate that oxygen clusters, namely, clustering-triggered emission (CTE), can well explain the inherent fluorescence of oligomeric siloxanes. Moreover, intermolecular hydrogen bonds are conducive to the aggregation of the molecular chains. Then, these bonds will facilitate the formation of oxygen clusters, which produce electron cloud overlap to form the unusual chromophores. In addition, the results suggest that the fluorescence intensity of oligomeric siloxanes enhances with increasing concentration. Furthermore, excitation-dependent emission behavior is observed when varying the excitation wavelength of oligomeric siloxanes. It is also found that the luminescence of oligomeric siloxanes could be effectively tuned by the solvent and metal ions.

Introduction

Organic luminescent materials have become a research hotspot due to their unique photophysical properties and broad applications in organic light-emitting diodes (OLEDs) [1], optoelectronic devices, drug delivery [2], chemo-/bioprobes [3], and cell imaging [4]. Conventional luminescent materials generally contain π-conjugated benzene rings or heterocyclic rings functioning as emitting units. Most of these organic luminogens show an aggregation-caused quenching (ACQ) effect, which immensely impedes their practical applications [5]. In 2001, Tang and coworkers reported a very interesting aggregation-induced emission (AIE) effect from derivatives of hexaphenylsilole, which overcomes the troublesome ACQ effect [6]. However, these organic luminogens commonly have undesirable drawbacks, such as poor solubility and biocompatibility, restricting their application fields.

Nonconventional luminescent polymers containing no classic chromophores have attracted growing attention because of their distinct advantages, such as environmental friendliness, excellent biocompatibility, facile synthesis, and structural tenability. More importantly, unorthodox luminescent macromolecules exhibited the typical AIE effect, rendering them perfect candidates for biological and medical applications. In recent years, various luminogens without orthodox chromophores have been found to show extraordinary intrinsic luminescence [7–9]. Generally, these luminescent polymers include electron-rich heteroatoms, such as nitrogen (N) [10–23], oxygen (O) [24], sulfur (S) [25], unsaturated C = O [26–29], and C≡N [30]. Very recently, a number of siloxane-containing compounds without conventional fluorescence units have also shown blue fluorescence, such as siloxane-poly(amidoamine) [31],

Supplementary information The online version of this article (https://doi.org/10.1038/s41428-019-0208-1) contains supplementary material, which is available to authorized users.

✉ Hongxia Yan
hongxiayan@nwpu.edu.cn

[1] MOE Key Laboratory of Material Physics and Chemistry, Shaanxi Key Laboratory of Macromolecular Science and Technology, School of Science, Northwestern Polytechnical University, 710129 Xi'an, PR China

[2] Key Laboratory of Polymer Science and Technology, Shaanxi Province, School of Science, Northwestern Polytechnical University, Chang'an district dong'xiang road 1, 710129 Xi'an, PR China

siloxane derivatives [32] and siloxane-containing poly (hydroxyurethane) (PHU) [33]. To date, several mechanisms have been proposed, including oxidation [34], formation of hydroxylamines [35], aggregation of oxime groups (C = N–OH) [9], and clustering of carbonyl groups [36]. In addition, our groups reported a series of fluorescent hyperbranched polysiloxanes that have different functional groups, for example, carbon-carbon double bonds and hydroxyl groups, epoxy and hydroxyl groups, or primary amine and hydroxyl groups [37, 38]. Our preliminary studies show that their luminescence was closely associated with the terminal groups. To obtain insight into the mechanism of emission, the design and preparation of siloxane-containing polymers are extremely necessary.

In this paper, we successfully synthesized two types of oligomeric siloxanes by employing glycerol (GCL) and 1,4-Butanediol (BDO) as the polyol source and 3-aminopropyl (diethoxy)methylsilane (APMDES) as the silicon source via a facile and straightforward polycondensation reaction. The as-synthesized oligomeric siloxanes show unexpected blue fluorescence under 365 nm UV irradiation. Therefore, the inherent fluorescence properties of oligomeric siloxanes were systematically investigated. Moreover, the luminescence mechanism of oligomeric siloxanes was thoroughly explored.

Experimental procedures

Measurements

Proton nuclear magnetic resonance (^{1}H NMR, ^{13}C NMR) spectra were obtained on a Bruker Advance 400 spectrometer at 25 °C utilizing DMSO-d_6 as solvent. Molecular weight distributions were determined using gel permeation chromatography (GPC, waters 1515). Ultrapure water was used as the mobile phase, and the measurement was run at a flow rate of 1 mL min^{-1}. The GPC system was equipped with a Waters 2414 refractive index detector and a column system (Styragel HT 3, 7.8 × 300 mm, Ireland). Fourier transform infrared (FTIR) spectra were recorded on a Bruker Tensor 27 infrared spectrophotometer within the 4000–400 cm^{-1} region using the KBr pellet technique. The distillates were analyzed using a SP-6890 (Lu nan, Shandong) gas chromatograph (GC) equipped with an FID detector and a capillary column (SE-54), where the initial temperature of 70 °C was held for 2 min, then raised to 240 °C under a N_2 flow rate of 20 mL min^{-1} and kept for 6 min. The temperature of the vaporization chamber and detector were maintained at 200 and 180 °C, respectively. Luminescence (excitation and emission) spectra of the samples were collected with a Hitachi F-4600 fluorescence spectrophotometer using a monochromated Xe lamp as an excitation source at room temperature. The slit widths of both excitation and emission were set at 5 nm, and the scan wavelength speed was 2400 nm min^{-1}. The fluorescence lifetime (FL) and absolute quantum yield (QY) of S1 at a concentration of 100 mg/mL were determined on a steady/transient-state fluorescence spectrometer equipped with an integrating sphere (FLS980, Edinburgh Instruments) using $BaSO_4$ as a reference. UV-vis spectra were acquired using a UV-Visible spectrophotometer (SHIMADZU UV-2550, Japan).

Materials

BDO, GCL and APMDES were purchased from Macklin Chemical Reagent Co., Ltd. Polyether amine (PEA) was provided by Dalian Liansheng Trading Co., Ltd. Methanol, ethanol, acetone, hydrochloric acid, N,N-dimethylformamide (DMF) and N-methyl-2-pyrrolidone (NMP) were purchased from Guangdong Guanghua Sci-Tech Co., Ltd. $FeCl_3$•$6H_2O$, $CoCl_2$•$6H_2O$, $CuCl_2$•$2H_2O$, $CdCl_2$, $ZnCl_2$ and $CaCl_2$ were purchased from Sinopharm Chemical Reagent Co., Ltd. All materials were used without further purification.

Synthesis of oligomeric siloxanes

Oligomeric siloxanes were synthesized via a one-pot method according to a literature procedure [37], and the synthesis process is described as follows: First, 27.9061 g of GCL (0.3 mol) and 59.1773 g of APMDES (0.3 mol) were charged into a 250 mL four-neck flask equipped with a N_2 gas inlet, a thermometer, a mechanical stirrer, a distilling setup and a water condenser. Then, the mixture was heated to 110 °C and kept at this temperature until some byproduct was distilled off. Subsequently, the temperature was continuously increased to 160 °C, and the distillate temperature was kept below 78 °C. The reaction system was held at 160 °C until the distillate temperature was lower than 55 °C. Afterwards, the mixture was collected in a vial after it was cooled to 60 °C. The mixture was dialyzed in ethanol for 12 h to remove the unreacted materials. Eventually, the oligomeric siloxane, denoted S1, was synthesized. Furthermore, the byproduct was named distillate-1.

The linear oligomeric siloxane (S2) was synthesized using BDO as a polyol, and the molar ratio of –OH to $–OC_2H_5$ was 1.1:1. The oligomeric siloxane was synthesized using 59.1773 g of APMDES (0.3 mol) and 30.3465 g of BDO (0.33 mol) based on the synthesis process of S1. The byproduct of S2 is marked as distillate-2. The crude product was dialyzed in ethanol for 12 h. The synthetic route for the oligomeric siloxanes is presented in Scheme 1.

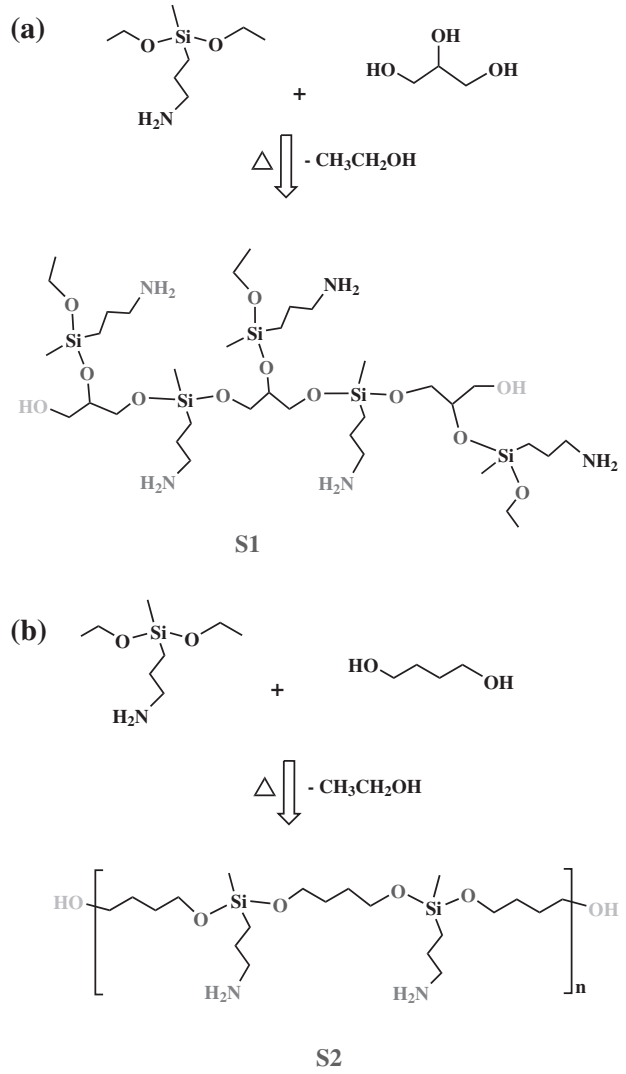

Scheme 1 Synthetic routes of (**a**) S1 and (**b**) S2

Results and discussion

Structural characterization of oligomeric siloxanes

The chemical structures of the oligomeric siloxanes were characterized by ^{1}H NMR, ^{13}C NMR, and FTIR. The ^{1}H NMR spectra of the raw materials, S1 and S2 are displayed in Fig. 1. From Fig. 1a, it can be seen that the proton peak of –CH_2–C<u>H</u>(OH)–CH_2– for GCL is not observed in S1, which demonstrates that the secondary alcohols of GCL are completely consumed. In addition, the proton peaks of –O–$C\underline{H}_2$–CH_3 and –O–CH_2–$C\underline{H}_3$ for APMDES are observed in S1, indicating that the ethoxy groups are present in S1, although the hydroxyl groups are in excess. GCL has two primary OH groups and one secondary OH group, which possess different reactivities toward transesterification reactions [39]. Additionally, the secondary OH groups preferentially reacted with $–OC_2H_5$, which has been confirmed by the DFT method in previous work [40].

The ^{1}H NMR spectrum of S1 is shown in Fig. 1b. The signals at 3.24–3.64 ppm are attributed to the protons of glycerol. The peaks at 0.51, 1.37, and 2.49 ppm correspond, respectively, to the –CH_2–$C\underline{H}_2$–Si, –$C\underline{H}_2$–CH_2–Si–, and NH_2–$C\underline{H}_2$–CH_2– groups. The chemical band at 0.06 ppm is assigned to the methyl group of Si–$C\underline{H}_3$. The peaks at 1.06 and 3.68 ppm are assigned to –O–CH_2–$C\underline{H}_3$ and –O–$C\underline{H}_2$–CH_3, respectively.

The ^{1}H NMR spectra of APMEDS, BDO and S2 are displayed in Fig. 1c, d. As shown in Fig. 1d, methylene group protons, namely, –$C\underline{H}_2$–$(CH_2)_2$–$C\underline{H}_2$–O–Si–, NH_2–$C\underline{H}_2$–CH_2–, –CH_2–$(C\underline{H}_2)_2$–CH_2–O–Si–, –$C\underline{H}_2$–CH_2–Si-, and –CH_2–$C\underline{H}_2$–Si–, are observed at 3.65, 2.75, 1.67, 1.49, and 0.52 ppm, respectively.

Figure 2a, b show the ^{13}C NMR spectra of APMDES, GCL and S1. As shown in Fig. 2b, the peaks at 72.91 and 63.48 ppm are ascribed to O–$\underline{C}H_2$– and –$\underline{C}$HOH–, respectively. The signals of the secondary carbons (–CH_2–) at 14.81, 27.25, 45.14, and 56.46 ppm correspond to –CH_2–$\underline{C}H_2$–Si–, –$\underline{C}H_2$–CH_2–Si–, –CH_2–$\underline{C}H_2$–NH_2, and –O–$\underline{C}H_2$–CH_3, respectively. The peaks at 18.97 and −0.29 ppm are assigned to the primary carbon (–$\underline{C}H_3$).

Figure 2c, d show the ^{13}C NMR spectra of APMDES, BDO and S2. From Fig. 2d, it can be seen that the signals at 62.23, 44.93, 29.92, 26.99, 14.6 and −0.67 ppm are associated with –$\underline{C}H_2$–$(CH_2)_2$–$\underline{C}H_2$–, NH_2–$(\underline{C}H_2)_2$–, CH_2–$(\underline{C}H_2)_2$–CH_2–, –$\underline{C}H_2$–CH_2–Si–, –CH_2–$\underline{C}H_2$–Si–, –Si–$\underline{C}H_3$, respectively.

The FTIR spectra of all the raw materials and polymers are plotted in Fig. 3. Figure 3a displays the spectra of GCL, APMDES and S1. The characteristic absorption peak at approximately 3365 cm^{-1} for GCL belongs to the –OH groups. In the APMDES spectrum, it can be seen that the significant absorption peaks at 1105 and 1076 cm^{-1} are assignable to the Si–O–C bonds. In particular, the characteristic absorption peak for the –OH groups in S1 is located at approximately 3359 cm^{-1}. In addition, the characteristic band at 1053 cm^{-1} for S2 is assigned to the Si–O–C bonds. Figure 3b shows the spectra of BDO, APMDES and S2. Likewise, the characteristic absorption bands at ~3365 and 3286 cm^{-1} arise from the $–NH_2$ groups, and the band at 1089 cm^{-1} originates from the Si–O–C bonds.

Additionally, the distillates produced during the polymerization reaction were detected using FTIR spectroscopy and gas chromatography to characterize the polymerization reaction (Fig. S1). Commercially available ethanol is used as a standard to analyze the distillates. As shown in Fig. S1a, the FTIR spectra of ethanol and the distillates possess practically the same peak shape. Moreover, the GC data further verify that the byproduct is ethanol, which

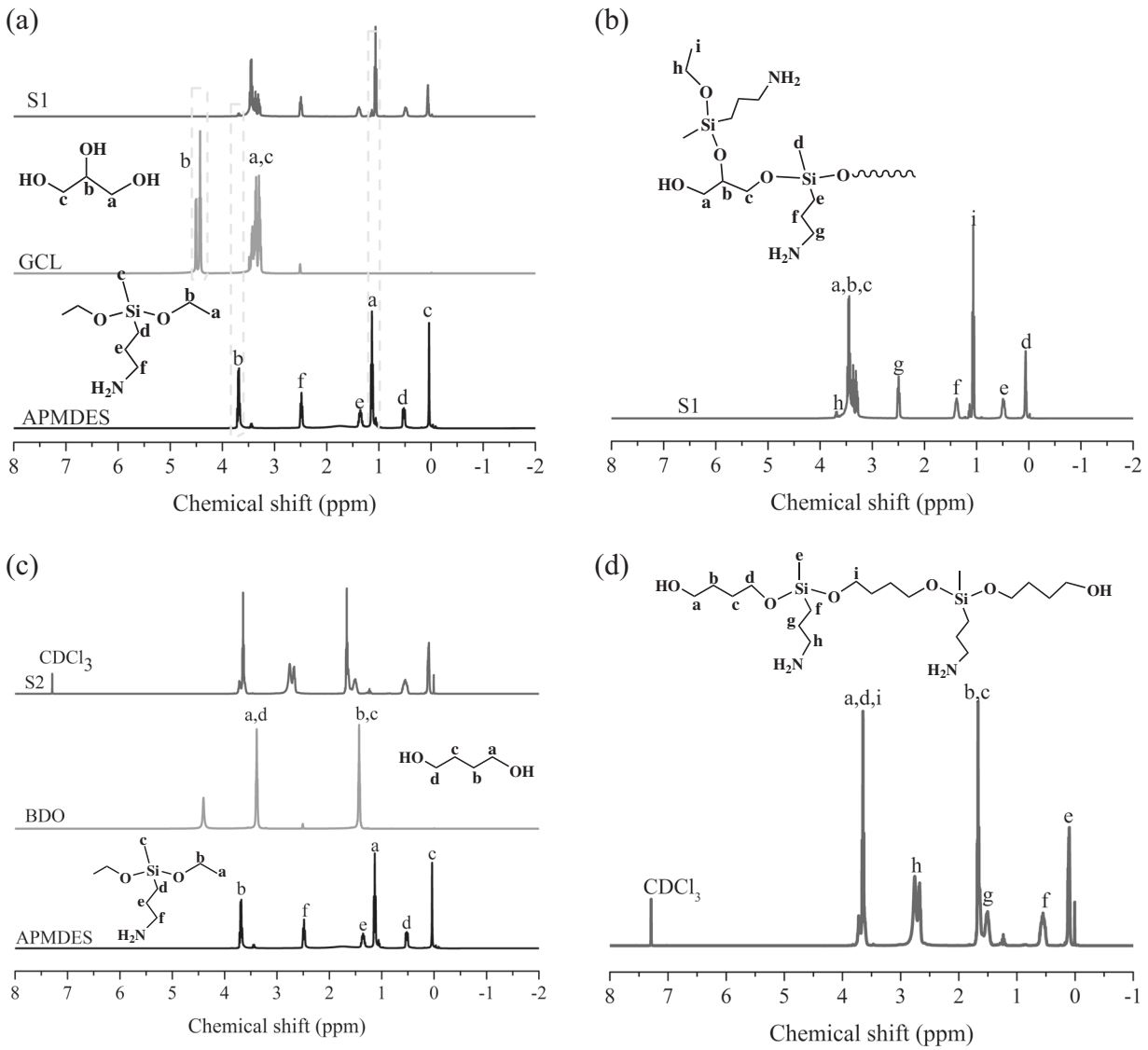

Fig. 1 **a** ^{1}H NMR spectra of APMDES, GCL and S1. **b** ^{1}H NMR spectrum of S1. **c** ^{1}H NMR spectra of APMDES, BDO and S2. **d** ^{1}H NMR spectrum of S2

illustrates that this reaction is feasible and that the desired polymers can be obtained successfully. The GPC curves of oligomeric siloxanes are presented in Fig. S2. From Table S1, it can be seen that the M_w values of S1 and S2 are 1797 and 1597 g/mol, respectively. These results indicate that oligomeric siloxanes S1 and S2 were successfully prepared under catalyst-free conditions.

Fluorescence properties of oligomeric siloxanes

To our surprise, the synthesized S1 and S2 are viscous and yellowish products under room light, while they can emit intense blue fluorescence under 365 nm UV irradiation (Fig. 4a, b), which demonstrates that they have representative AIE characteristics. Additionally, aqueous solutions of both S1 and S2 also exhibit blue fluorescence, and the fluorescence of the S1 solution is slightly stronger than that of S2 (Fig. 4c).

PL spectra of S1 and S2 aqueous solutions at different excitation wavelengths (λ_{ex}) are depicted in Fig. 5. As shown in Fig. 5a, b, as the λ_{ex} increases, the emission wavelengths (λ_{em}) of the S1 and S2 aqueous solutions show an obvious redshift, exhibiting excitation-dependent emission (EDE) behavior, which can be clearly observed from Fig. S3. This EDE behavior is strongly indicative of the existence of diverse emissive species, which has been recognized as a common characteristic of fluorescent hyperbranched polymers without conventional chromophores [41]. To visually observe the change in fluorescence color, we calculated the CIE (Commission Internationale d'Éclairage) coordinates of S1 and S2 at a concentration of 40 mg/mL in water after excitation at varying λ_{ex} based on

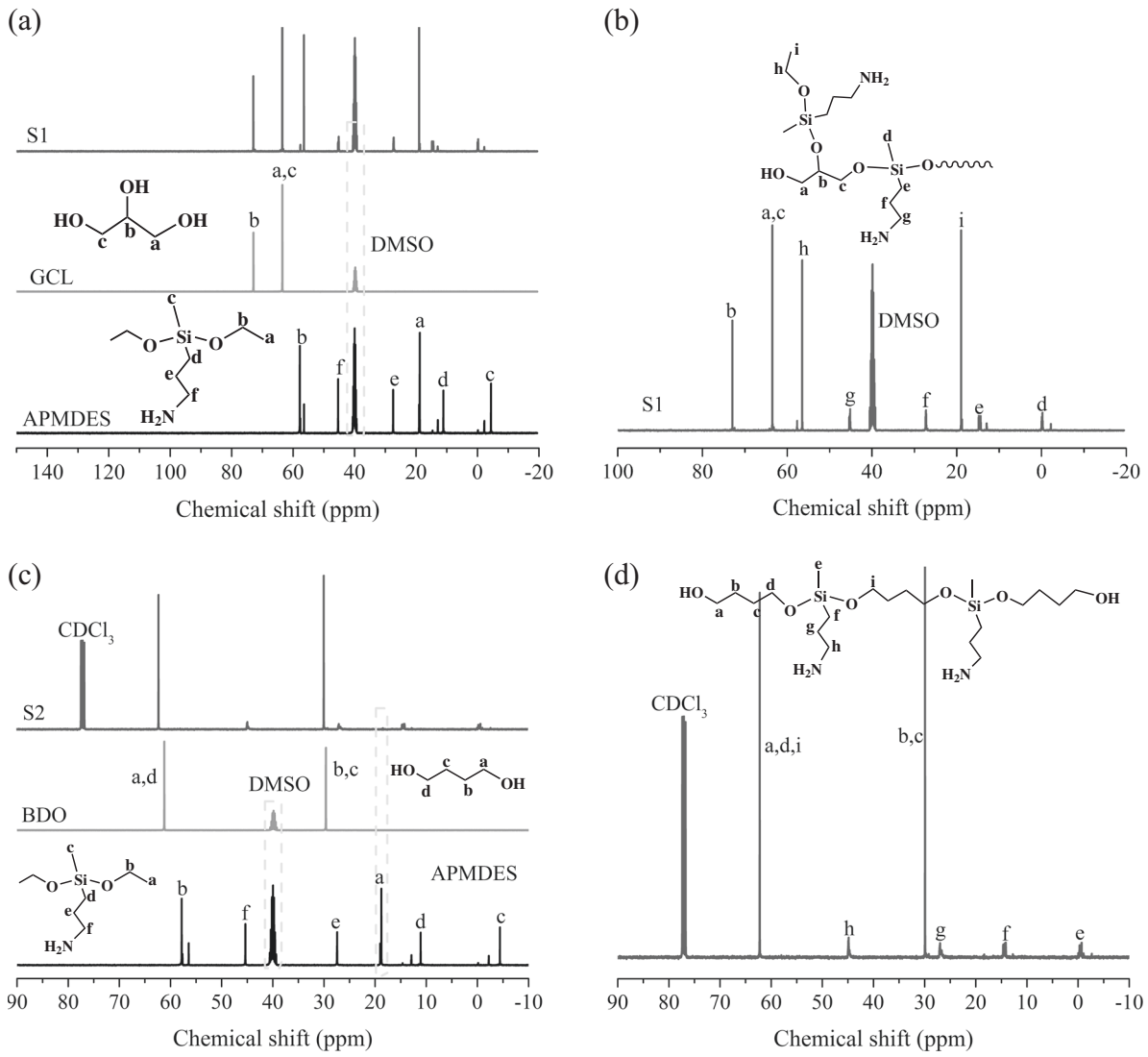

Fig. 2 **a** ^{13}C NMR spectra of APMDES, GCL and S1. **b** ^{13}C NMR spectrum of S1. **c** ^{13}C NMR spectra of APMDES, BDO and S2. **d** ^{13}C NMR spectrum of S2

the data in Tables S2 and S3. It is clearly observed that the fluorescence color emitted from the S1 and S2 solutions gradually changes from dark blue to light blue with increasing λ_{ex} (Fig. 5c, d).

Fluorescence spectra and UV-vis spectra of S1 solutions at different concentrations were acquired, as shown in Fig. 6. The absorption profile of the concentrated S1 solutions displays a peak at ~28 nm, while weak absorption of dilute S1 solution is observed. This absorption progressively enhances with increasing S1 concentration (Fig. 6a). The fluorescence spectra of the S1 solutions display that the PL intensity increases as the concentration increases, exhibiting significant concentration-dependent emission (CDE) behavior (Fig. 6b), which is similar to the behavior observed from other nontraditional luminogens [27]. The fluorescence signals of S1 solutions at 5–10 mg/mL are so low that no visible emission is observed (Fig. 6c). Observable emission is detected from a 20 mg/mL S1 solution, and further boosted emission is detected as the S1 concentration increases. These results demonstrate that the S1 chain segments are aggregated in highly concentrated solutions.

To explore the luminescence centers of the oligomeric siloxanes, we designed and synthesized linear siloxane oligomer S2. The fluorescence properties of S2 solutions were carefully studied. The UV-vis spectra of S2 solutions with different concentrations exhibit an absorption peak at ~294 nm, which is slightly redshifted compared to that of S1 solutions (Fig. 7a). As the S2 concentration increases, the absorption also gradually increases. In addition, the fluorescence spectra of S2 solutions at various concentrations show that the PL intensity of S2 solutions increases with increasing concentration, also showing CDE behavior (Fig. 7b). As shown in Fig. 7c, visible blue fluorescence is

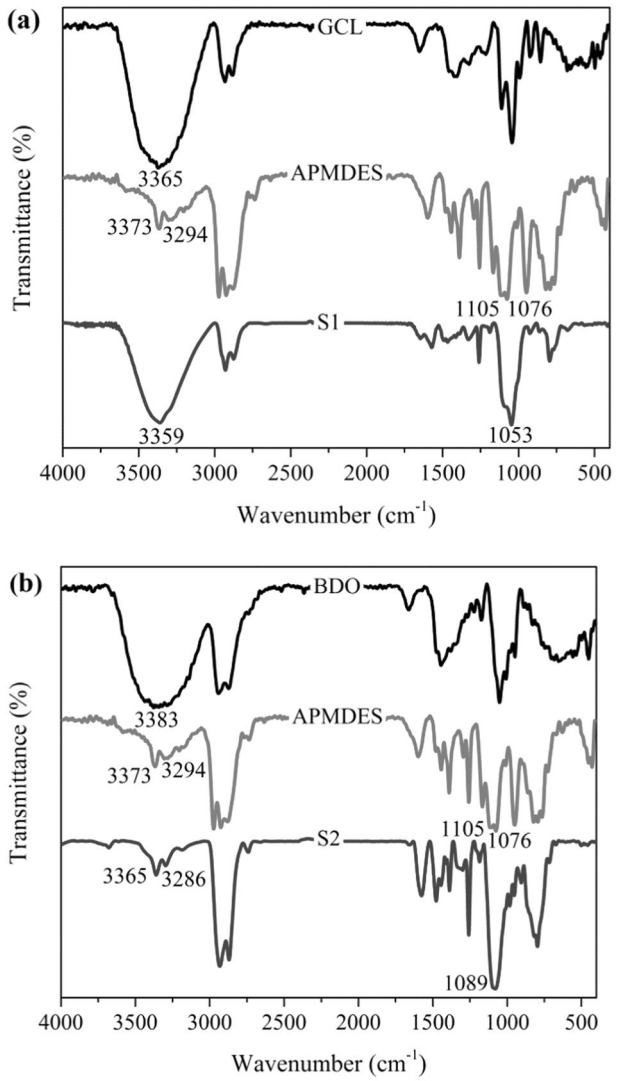

Fig. 3 (**a**) FTIR spectra of GCL, APMDES and S1. (**b**) FTIR spectra of BDO, APMDES, and S2

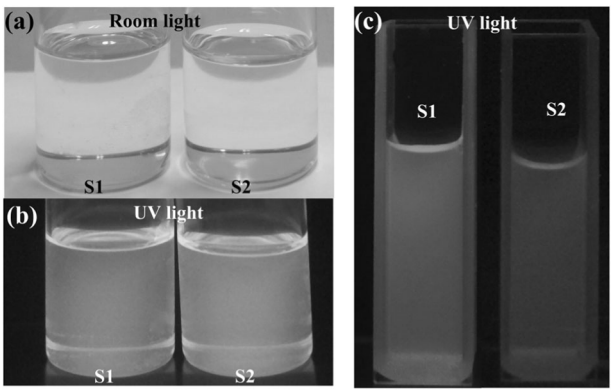

Fig. 4 Photographs of oligomeric siloxanes in a pure state under room light (**a**) and 365 nm UV light (**b**) and their aqueous solutions ($C = 100$ mg/mL) under 365 nm UV light (**c**)

not observed in dilute S2 solution, while the fluorescence becomes brighter in the concentrated S2 solution, which also indicates the presence of aggregates in the concentrated S2 solution.

Fluorescence mechanism of oligomeric siloxanes

To the best of our knowledge, the exploration of the fluorescence mechanism of nontraditional luminescent polymers is a difficult problem because of their complex structures. The inherent fluorescence from the hyperbranched polyether inspires us to design simpler polymers that help reveal the underlying fluorescence mechanism [24]. Therefore, we designed and prepared oligomeric siloxanes as simple compounds to study the intrinsic fluorescence mechanism. Through the abovementioned investigation, it was found that both S1 and S2 could emit blue fluorescence in the pure state and highly concentrated state because of the aggregation of molecular chains. Both S1 and S2 consist of a Si–O–C skeleton. The common aspect of S1 and S2 is that they have oxygen, amino and hydroxyl groups, which may act as potential fluorescence units [42]. Yuan and colleagues have reported that the intrinsic emission of nonaromatic amino acids and poly (amino acids) can be ascribed to the clustering-triggered emission (CTE) mechanism [43].

Based on the above results and analysis, the unique fluorescence of oligomeric siloxanes can also be well explained via oxygen clustering, namely, the CTE mechanism. To verify the CTE mechanism of oligomeric siloxanes, we performed theoretical calculations by using the density functional theory (DFT) method at the B3LY/6–31G(d) level. To simplify the calculation, the first-generation S2 molecule is used as the model compound. As shown in Fig. 8a, intermolecular hydrogen bonds could form between four first-generation S2 molecules. The bond distances of Si–O…H–N, Si–O…H–O and Si–O…H–C are 2.2359, 2.9687, and 2.8389 Å, respectively. Moreover, H–O…H–C hydrogen bonds of could also form, which are marked by b (2.4682 Å), d (2.9062 Å), and e (2.9878 Å). These intermolecular hydrogen bonds are beneficial for aggregation of the molecular chains and then promote the formation of oxygen clusters. The HOMO-LUMO energy levels of various conformations of the first-generation S2 molecules were calculated (Fig. S4), and the results are shown in Table S4. The band gap energy gradually decreases as the number of molecules increases, which further suggests that the molecular chains of oligomeric siloxanes aggregate with increasing molecule number, leading to shortening of the distance between oxygen atoms. Short O···O contact could form oxygen clusters, causing their electron clouds to overlap and form unusual chromophores.

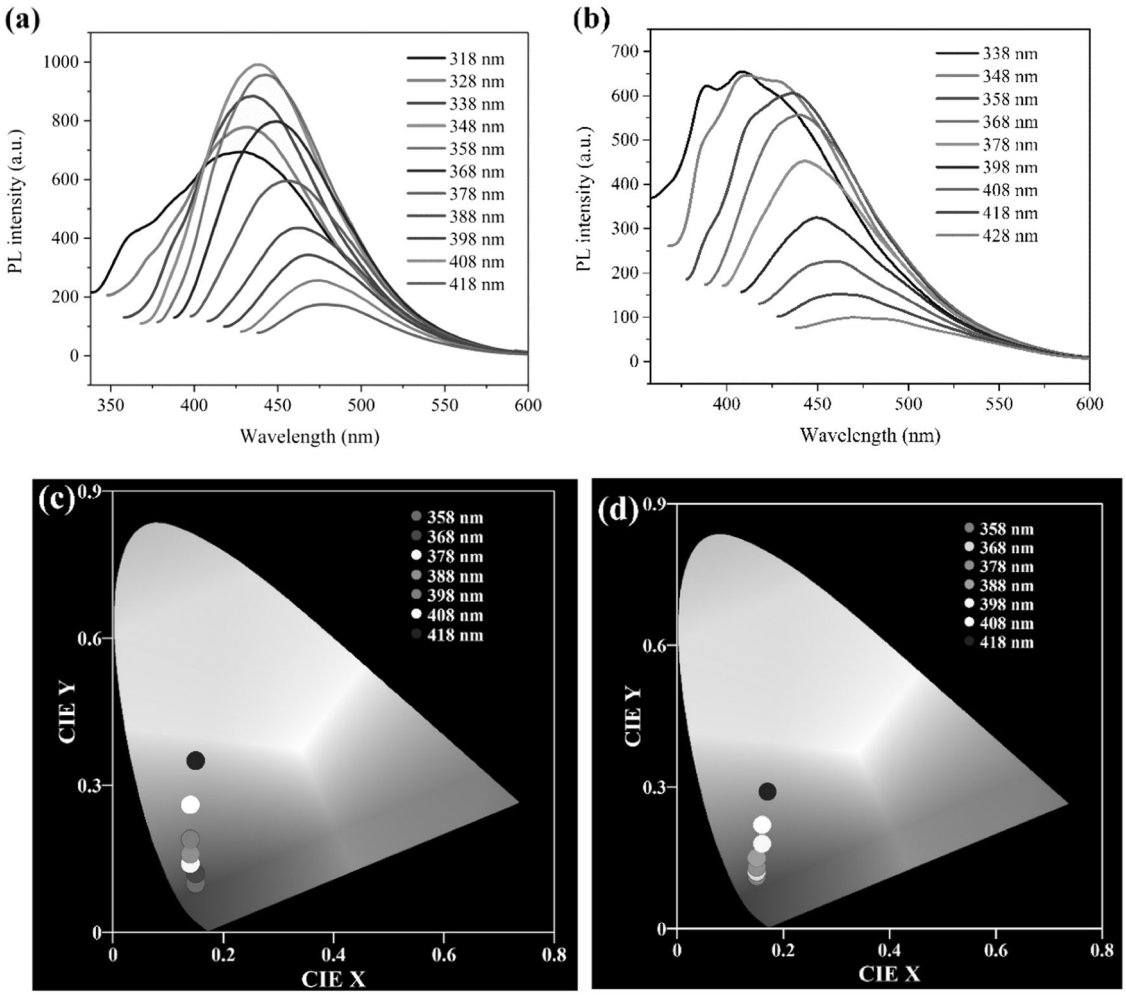

Fig. 5 PL spectra of S1 (**a**) and S2 (**b**) solutions with different excitation wavelengths. CIE chromaticity coordinates calculated from the emission spectra of S1 (**c**), and S2 (**d**) solutions after excitation at varying λ_{ex} values ($C = 100$ mg/mL)

In a dilute solution, polymer chains of S1 and S2 are well extended and isolated. As a result, it is very difficult to excite these species because of the absence of enough aggregation (Fig. 8b). Both the S1 and S2 solutions of 5 mg/mL could not emit visible fluorescence when excited by a 365 nm UV lamp. In concentrated solution, however, the distance between molecular chains of both S1 and S2 decreases, and the flexible molecular chains can approach each other and easily form multiple intermolecular hydrogen bonds. Under the action of intermolecular hydrogen bonding, the oligomer chains are aggregated, thereby forming dense oxygen clusters. In the formed oxygen clusters, electron cloud overlap could be produced by the short O···O contacts, which rigidifies the conformation. Consequently, the intra-/intermolecular bond rotations and vibrations could be reduced, resulting in more radiative decays of the singlet excitons. Subsequently, the highly concentrated solutions of S1 and S2 as well as pure S1 and S2 can give rise to the much brighter luminescence when excited with 365 nm UV irradiation.

We also measured the fluorescence of S1 and S2 solutions at the same concentration, as shown in Fig. S5. The maximum λ_{em} values of S1 and S2 solutions are at ~438 and 412 nm, respectively, when excited by the same λ_{ex}. Moreover, compared with the maximum λ_{em} of S2 solution, the maximum λ_{em} of S1 solution is redshifted by 26 nm, and the PL intensity of S1 is higher than that of S2. In the following, we summarize two reasons that can explain this phenomenon. On one hand, the conformation of S1 could more easily rigidify than that of the linear S2 as a result of S1 having a branched backbone, which is opposite to the fluorescence of polyethylenimines [13]. This phenomenon shows that the compact hyperbranched backbone is extremely important to the fluorescence of polymers containing merely oxygens [44]. On the other hand, S1 possesses more oxygen groups than S2, so more dense oxygen clusters can be formed in the concentrated solutions and pure state.

The flexibility of the Si–O bond may play an important role in the aggregation of the S1 and S2 molecular chains

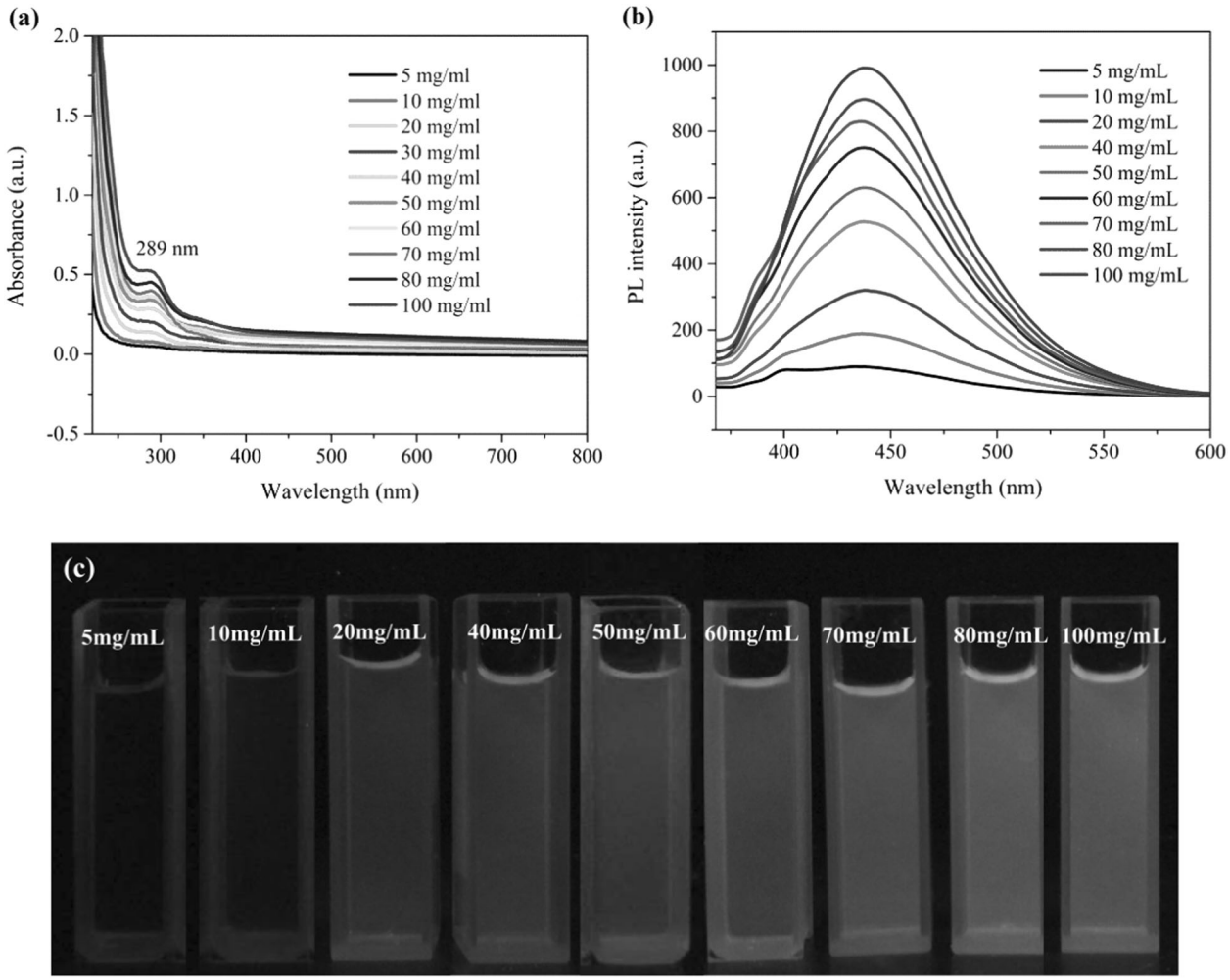

Fig. 6 **a** UV-vis spectra, b PL spectra ($\lambda_{ex} = 348$ nm), and **c** photographs of S1 ($\lambda_{ex} = 365$ nm) solutions at different concentrations

and the formation of oxygen clusters [31]. If the oligomers do not contain Si–O bonds, will they still emit fluorescence? To answer this question, we performed detailed tests on the fluorescence of a commercially available polyether amine (PEA) with only a C–O skeleton. The ^{1}H NMR spectrum of PEA is shown in Fig. S6. As we know, PEA contains a simple polyether backbone as well as one amino group at its terminal, as presented in Fig. 9a. It has been believed that PEA is not luminescent. However, pure PEA without any conventional chromophores gives impressive and weak blue fluorescence under 365 nm UV light, implying that the C–O chains of PEA could also aggregate in the pure state, which is similar to S1 and S2. The PL spectra of PEA solutions with different concentrations display that the PL intensity increases with increasing concentration (Fig. 9b), indicating that the PEA chains aggregate in highly concentrated solution. In particular, EDE behavior is also observed in PEA solution (Fig. 9c). Two emission bands at ~411 and 433 nm are observed in PEA solutions, demonstrating the existence of multiple emissive species. With increasing λ_{ex}, the PL intensity of PEA first increases, while the λ_{em} red-shifts slightly until their maximal λ_{em}. Afterwards, the PL intensity decreases, while the λ_{em} retains almost constant (Fig. 9d). PEA bearing only oxygen and NH_2 groups can emit weak fluorescence. Therefore, this unexpected fluorescence of PEA is apparently attributable to oxygen clusters. Specifically, the possible intermolecular hydrogen bonds, such as H–O…H–C and C–O…H–N, could aggregate the molecular chains (C–O) and subsequently facilitate the formation of oxygen clusters. In the formed oxygen clusters, electron cloud overlap is produced and then rigidifies the molecular conformation, which inhibits non-radiative deactivation, leading to the emission of weak fluorescence from pure PEA. Therefore, it is reconfirmed that oxygen clustering is accountable for the fluorescence of nonconjugated oligomeric siloxanes, PEA, and even other nonconjugated luminescent polymers containing merely oxygen moieties. More importantly, intermolecular hydrogen bonds are highly key to the fluorescence of unconventional luminescent polymers.

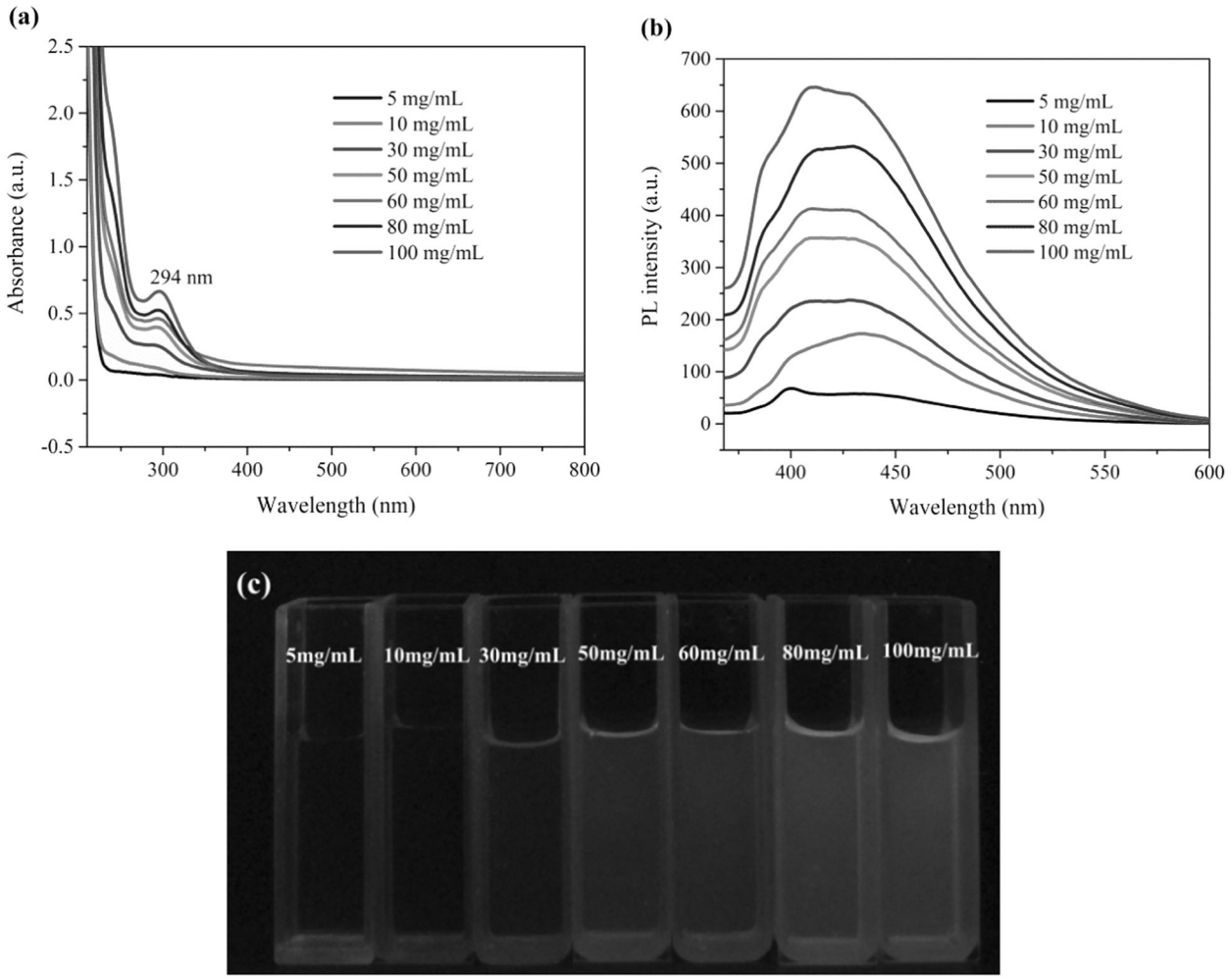

Fig. 7 **a** UV-vis spectra, **b** PL spectra ($\lambda_{ex} = 348$ nm), and **c** fluorescence images of S2 ($\lambda_{ex} = 365$ nm) solutions at different concentrations

QY and FL study

The QY and FL of the S1 solution were measured, as shown in Fig. 10. The decay curves of S1 solution are fitted by utilizing double exponential functions *R(t)* based on a non-least-squares analysis through the equation $R(t) = B_1\exp(-t/\tau_1) + B_2\exp(-t/\tau_2)$, where B_1 and B_2 are the fractional contributions of the time-resolved decay lifetime of τ_1 and τ_2, respectively (Table S5). The average fluorescence lifetime (τ_{avg}) of S1 solution was computed via $\tau_{avg} = (B_1\tau_1^2 + B_2\tau_2^2)/(B_1\tau_1 + B_2\tau_2)$. The τ_{avg} of S1 solution is calculated to be 5.87 ns (Fig. 10a). In addition, the QY of S1 solution is measured as 4.20% (Fig. 10b), which is similar to the QY values of 4.61% [45] and 3.68% reported for hyperbranched polysiloxanes [37].

Effect of the organic solvent

The resultant S1 has good solubility in water due to its hydrophilic nature. It can also dissolve in common organic solvents such as acetone, ethanol, methanol, DMF, and NMP. The fluorescence of S1 in various solvents was studied, and the result is shown in Fig. 11a. The fluorescence of S1 in diverse solvents shows solvent-dependent emission (SDE) behavior, which is also observed from other unconventional polymers [35]. The fluorescence intensity of S1 in acetone is the strongest, while the lowest fluorescence intensity is in DMF. Moreover, S1 shows much brighter blue luminescence in acetone than in DMF (Fig. S7). In addition, it can be clearly seen that there are two emission peaks at 390 and 411 nm and one shoulder peak at 438 nm in NMP and DMF, whereas there is one emission peak in the other solvents. A possible reason for this phenomenon is that the solvents could induce the aggregation of the molecular chains, so different PL intensities and emission wavelengths are observed in diverse solvents. Acetone having a weaker polarity may participate in the aggregation of the S1 molecular chains and then physically change the configuration of S1 [46, 47]. While S1 is not the same in NMP and DMF with electron-rich atoms as in acetone, these solvents could also aggregate the S1 molecular chains, which may form different aggregates, resulting in multiple emission peaks and a blueshift in the maximum λ_{em}.

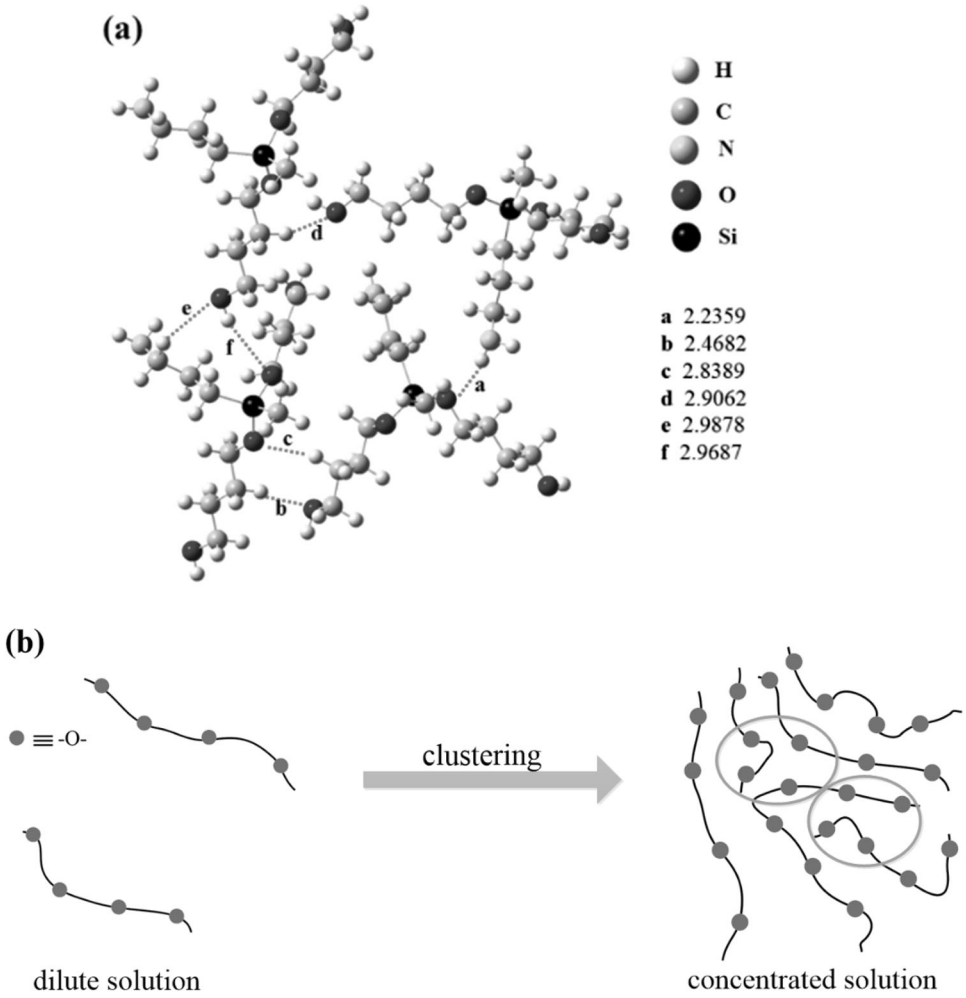

Fig. 8 **a** Optimized conformations of first-generation S2 molecules. **b** Schematic illustration of oligomeric siloxane molecules in dilute solutions and concentrated solutions

It is very interesting that the color of S1 in acetone [47] turned from colorless to yellow when S1 was dissolved in acetone for 0–26 days (Fig. S8). To our great surprise, the emission peak of S1 shows a gradual bathochromic shift from 434 to 465 nm accompanied by a decrease in the fluorescence intensity after the sample was dissolved in acetone for days (Fig. 11b). In addition, Feng and colleagues have also reported a similar phenomenon for Si-PAMAM, and acetone is very difficult to remove owing to the formation of intramolecular hydrogen bonds [46]. Hence, we consider that the small molecule acetone is possibly involved in the emission process of S1, which leads to changes in the fluorescence properties.

Influence of the pH and metal ions

A pH-dependent emission phenomenon has been observed in nontraditional luminescent polymers [16, 19]. Therefore, the fluorescence of aqueous S1 solutions with different pH values was measured, as shown in Fig. 12a. The fluorescence of S1 aqueous solutions exhibits better pH stability than that of unconventional fluorescent poly(amino esters) [22]. The initial pH value of the S1 aqueous solution without any acidification is ~11.88. As the pH is lowered to 9.24, the fluorescence intensity of S1 solution significantly increases and reaches the highest value. This phenomenon could be attributed to the presence of free OH^-, which may strengthen the intermolecular forces and thus make the structure of S1 more rigid, resulting in an enhancement in fluorescence. Upon further adjusting the pH values of S1 solutions to acidic conditions from 6.76 to 1.22, the fluorescence is hardly changed, implying that the aggregation of molecular chains of S1 is not altered in acidic environments.

It is well-known that Fe^{3+} is closely related to many diseases, such as anemia, Parkinson's disease, and malaria. Hyperbranched polyether and poly(ethylene glycol) having only nonconventional chromophores are sensitive to metal cations [24, 48]. Therefore, the stimulus response of the luminescence of 20 mg/mL S1 aqueous solutions was measured with various metal cations ($AlCl_3$, $ZnCl_2$, $CdCl_2$, $CoCl_2$, $CuCl_2$, $FeCl_3$), as shown in Fig. 12b. The fluorescence intensity of the S1 solution decreases when metal ions are added. However, the extent of the reduction in fluorescence intensity depends remarkably on the type of metal

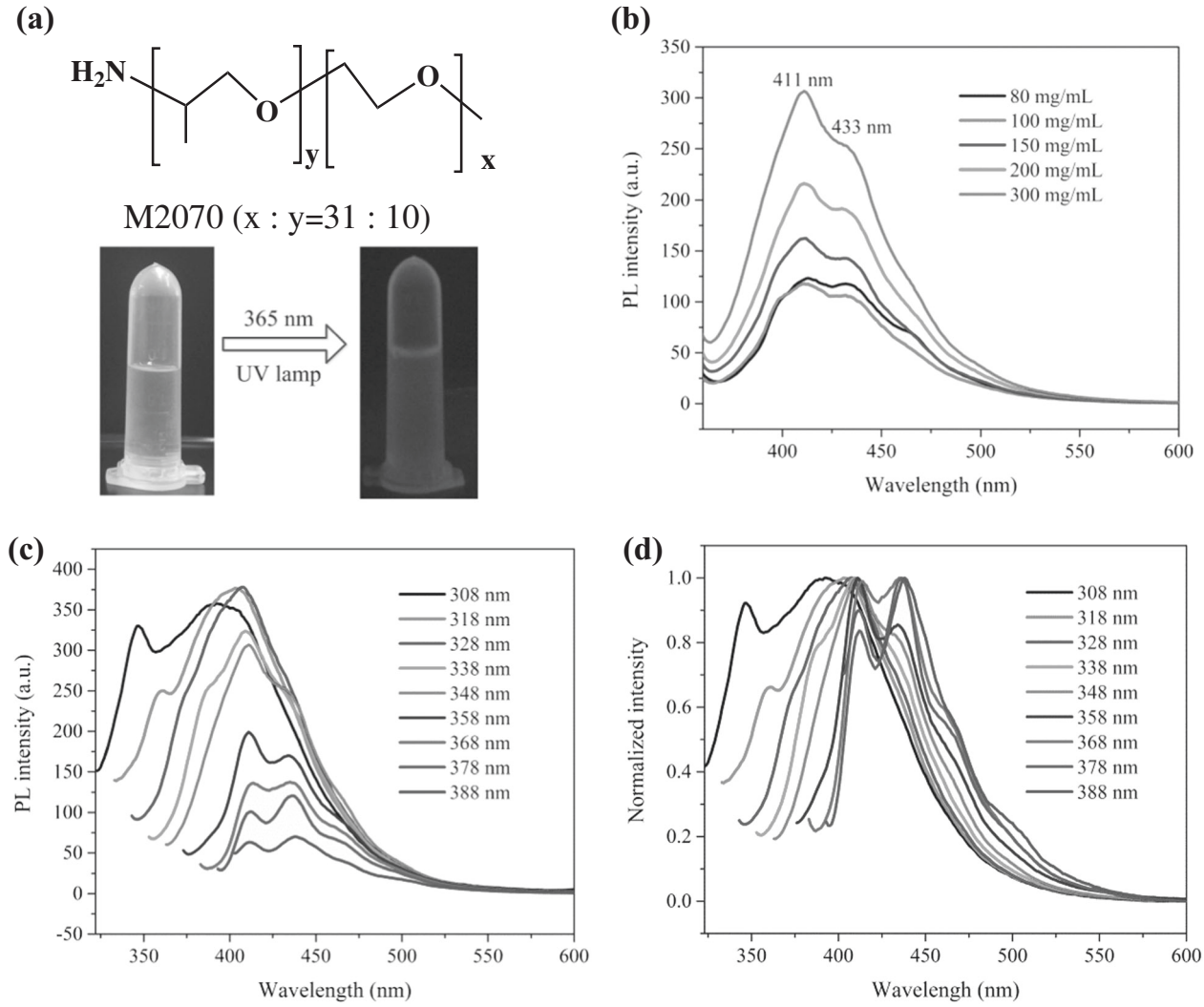

Fig. 9 **a** PEA structure and photographs under room light and UV light. **b** PL spectra of PEA solutions under different concentrations ($\lambda_{ex} = 348$ nm). **c** PL spectra of PEA solution under various λ_{ex} values. **d** Normalized emission intensity of PEA solution ($C = 300$ mg/mL)

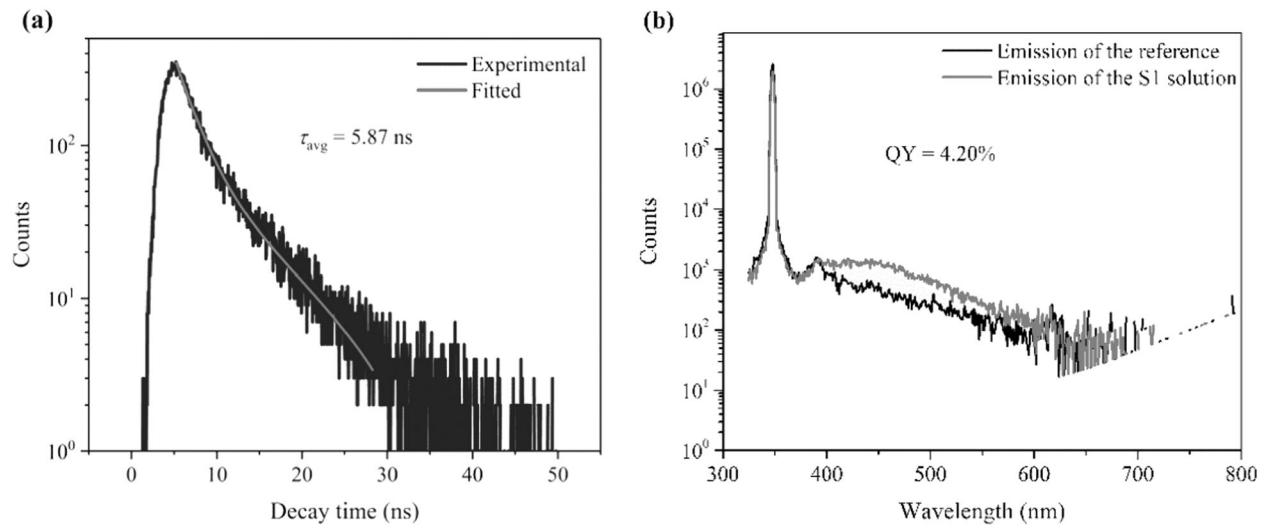

Fig. 10 **a** Transient photoluminescence decay curve of S1 solution at 438 nm after excitation at 348 nm. **b** QY of S1 solution excited at 348 nm ($C = 100$ mg/mL)

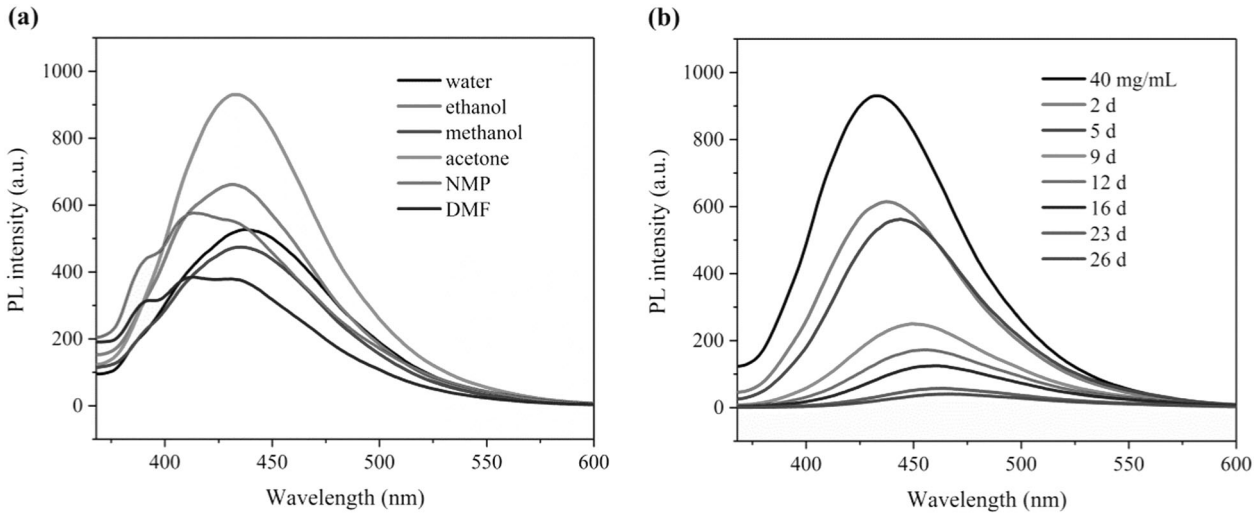

Fig. 11 **a** PL spectra of S1 solutions in various solvents. **b** PL spectra of S1 solutions in acetone ($C = 40$ mg/mL, $\lambda_{ex} = 348$ nm)

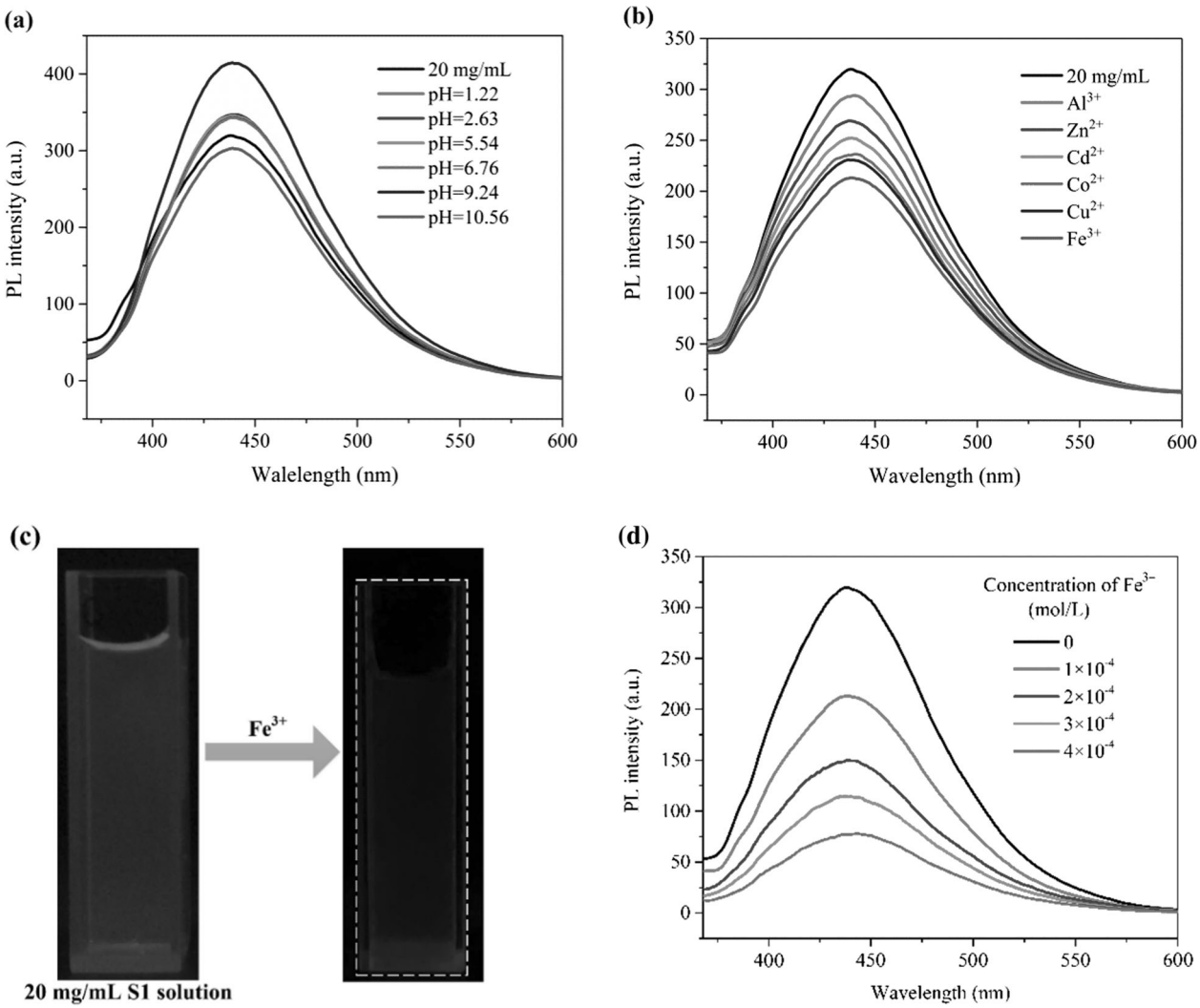

Fig. 12 PL spectra of S1 solutions **a** at varying pH values and **b** in the presence of different metal ions at the same concentration (1.0×10^{-4} mol/L). **c** Photographs of S1 solution (20 mg/mL) in the absence (left) and presence (right) of Fe^{3+} taken under 365 nm UV light. **d** PL spectra of S1 solutions with different concentrations of Fe^{3+}

ion. The PL intensity of S1 decreases in the order of Al^{3+}, Zn^{2+}, Cd^{2+}, Co^{2+}, Cu^{2+}, and Fe^{3+}. As observed in Fig. 12c, the fluorescence of 20 mg/mL S1 solution almost disappeared when Fe^{3+} was added due to its paramagnetic property [49, 50]. In addition, the PL intensity of S1 solutions with different Fe^{3+} concentrations was also recorded. With increasing Fe^{3+} concentrations, the PL intensity of S1 gradually decreases. At a Fe^{3+} concentration of 4×10^{-4} M, the PL intensity of S1 decreases 76%, which demonstrates that S1 can be applied as a potential fluorescent probe for detecting Fe^{3+}.

Conclusion

In summary, two kinds of oligomeric siloxanes were synthesized via a facile and convenient one-pot transesterification reaction for the first time. Strong blue luminescence can be observed even with the naked eye from synthetic S1 and S2 when they are irradiated by 365 nm UV light. We propose that oxygen clusters, namely, CTE, are responsible for the fluorescence of oligomeric siloxanes. Moreover, intermolecular hydrogen bonds could induce the aggregation of the molecular chains, which promotes the formation of oxygen clusters. The fluorescence intensities of both S1 and S2 display CDE and EDE behaviors. Furthermore, organic solvent and metal ions can dramatically tune the photoluminescent property of S1. More importantly, stable fluorescence of S1 is observed at different pH values. This work not only uncovers the fluorescence mechanism of nonconjugated luminescent polymers but also provides a new perspective for designing additional novel luminescent materials.

Acknowledgements This work is sponsored by the National Natural Science Foundation of China (21875188), Natural Science Basic Research Plan in Shaanxi Province of China (Program No. 2018JM2024) and the Innovation Foundation for Doctor Dissertation of Northwestern Polytechnical University (CX201719).

Compliance with ethical standards

Conflict of interest The authors declare on conflict of interest.

References

1. Kelley TW, Baude PF, Gerlach C, Ender DE, Muyres D, Haase MA, et al. Recent progress in organic electronics: materials, devices, and processes. Chem Mater. 2004;16:4413–223.
2. Qiu F, Wang D, Zhu Q, Zhu L, Tong G, Lu Y, et al. Real-time monitoring of anticancer drug release with highly fluorescent star-conjugated copolymer as a drug carrier. Biomacromolecules. 2014;15:1355–64.
3. Prodi L, Bolletta F, Montalti M, Zaccheroni N. Luminescent chemosensors for transition metal ions. Coord Chem Rev. 2000;205:59–83.
4. Yang W, Pan CY, Liu XQ, Wang J. Multiple functional hyperbranched poly(amido amine) nanoparticles: synthesis and application in cell imaging. Biomacromolecules . 2011;12:1523–31.
5. Chen G, Li W, Zhou T, Peng Q, Zhai D, Li H, et al. Conjugation-induced rigidity in twisting molecules: filling the gap between aggregation-caused quenching and aggregation-induced emission. Adv Mater. 2015;27:4496–501.
6. Luo J, Xie Z, Lam JWY, Cheng L, Chen H, Qiu C, et al. Aggregation-induced emission of 1-methyl-1,2,3,4,5-pentaphenylsilole. Chem commun. 2001;18:1740–1.
7. Shang C, Wei N, Zhuo H, Shao Y, Zhang Q, Zhang Z, et al. Highly emissive poly(maleic anhydride-alt-vinyl pyrrolidone) with molecular weight-dependent and excitation-dependent fluorescence. J Mater Chem C. 2017;5:8082–90.
8. Ye R, Liu Y, Zhang H, Su H, Zhang Y, Xu L, et al. Non-conventional fluorescent biogenic and synthetic polymers without aromatic rings. Polym Chem. 2017;8:1722–7.
9. Zhang Q, Mao Q, Shang C, Chen YN, Peng X, Tan H, et al. Simple aliphatic oximes as nonconventional luminogens with aggregation-induced emission characteristics. J Mater Chem C. 2017;5:3699–705.
10. Wang D, Imae T. Fluorescence emission from dendrimers and its pH dependence. J Am Chem Soc. 2004;126:13204–5.
11. Lee WI, Bae Y, Bard AJ. Strong blue photoluminescence and ECL from OH-terminated PAMAM dendrimers in the absence of gold nanoparticles. J Am Chem Soc. 2004;126:8358–9.
12. Jasmine MJ, Kavitha M, Prasad E. Effect of solvent-controlled aggregation on the intrinsic emission properties of PAMAM dendrimers. J Lumin. 2009;129:506–13.
13. Pastor-Pérez L, Chen Y, Shen Z, Lahoz A, Stiriba SE. Unprecedented blue intrinsic photoluminescence from hyperbranched and linear polyethylenimines: polymer architectures and pH-effects. Macromol Rapid Commun. 2007;28:1404–9.
14. Song G, Lin Y, Zhu Z, Zheng H, Qiao J, He C, et al. Strong fluorescence of poly(N-vinylpyrrolidone) and its oxidized hydrolyzate. Macromol Rapid Commun. 2015;36:278–85.
15. Jayamurugan G, Umesh CP, Jayaraman N. Inherent photoluminescence properties of poly(propyl ether imine) dendrimers. Organ Lett. 2008;10:9–12.
16. Restani RB, Morgado PI, Ribeiro MP, Correia IJ, Aguiar-Ricardo A, Bonifácio VD. Biocompatible polyurea dendrimers with pH-dependent fluorescence. Angew Chem Int Ed. 2012;51:5162–5.
17. Yang W, Pan CY. Synthesis and fluorescent properties of biodegradable hyperbranched poly(amido amine)s. Macromol Rapid Commun. 2009;30:2096–101.
18. Lin Y, Gao JW, Liu HW, Li YS. Synthesis and characterization of hyperbranched poly(ether amide)s with thermoresponsive property and unexpected strong blue photoluminescence. Macromolecules. 2009;42:3237–46.
19. Shiau SF, Juang TY, Chou HW, Liang M. Synthesis and properties of new water-soluble aliphatic hyperbranched poly(amido acids) with high pH-dependent photoluminescence. Polymer. 2013;54:623–30.
20. Wu D, Liu Y, He C, Goh SH. Blue photoluminescence from hyperbranched poly(amino ester)s. Macromolecules. 2005;38:9906–9.
21. Chen X, Liu X, Lei J, Xu L, Zhao Z, Kausar F, et al. Synthesis, clustering-triggered emission, explosive detection and cell imaging of nonaromatic polyurethanes. Mol Sys Des Eng. 2018;3:364–75.
22. Du Y, Yan HX, Niu S, Bai L, Chai F. Facile one-pot synthesis of novel water-soluble fluorescent hyperbranched poly(amino esters). RSC Adv. 2016;6:88030–7.

23. Chen H, Dai W, Huang J, Chen S, Yan XH. Construction of unconventional fluorescent poly(amino ester) polyols as sensing platform for label-free detection of Fe^{3+} ions and l-cysteine. J Mater Sci. 2018;53:15717–25.
24. Miao X, Liu T, Zhang C, Geng X, Meng Y, Li X. Fluorescent aliphatic hyperbranched polyether: chromophore-free and without any N and P atoms. Phys Chem Chem Phys. 2016;18:4295–9.
25. Zhang Z, Feng S, Zhang J. Facile and efficient synthesis of carbosiloxane dendrimers via orthogonal click chemistry between thiol and ene. Macromol Rapid Commun. 2016;37:318–22.
26. Zhao E, Lam JW, Meng L, Hong Y, Deng H, Bai G, et al. Poly [(maleic anhydride)-alt-(vinyl acetate)]: a pure oxygenic nonconjugated macromolecule with strong light emission and solvatochromic effect. Macromolecules. 2014;48:64–71.
27. Du Y, Feng Y, Yan HX, Huang W, Yuan L, Bai L. Fluorescence emission from hyperbranched polycarbonate without conventional chromohpores. J Photo Photobio A. 2018;364:415–23.
28. Huang W, Yan HX, Niu S, Du Y, Yuan L. Unprecedented strong blue photoluminescence from hyperbranched polycarbonate: From its fluorescence mechanism to applications. J Polym Sci Poly Chem. 2017;55:3690–6.
29. Zhou X, Luo W, Nie H, Xu L, Hu R, Zhao Z, et al. Oligo(maleic anhydride)s: a platform for unveiling the mechanism of cluster-oluminescence of non-aromatic polymers. J Mater Chem C. 2017;5:4775–9.
30. Zhou Q, Cao B, Zhu C, Xu S, Gong Y, Yuan WZ, et al. Clustering-triggered emission of nonconjugated polyacrylonitrile. Small . 2016;12:6586–92.
31. Lu H, Feng L, Li S, Zhang J, Lu H, Feng SY. Unexpected strong blue photoluminescence produced from the aggregation of unconventional chromophores in novel siloxane-poly(amidoamine) dendrimers. Macromolecules. 2015;48:476–82.
32. Lu H, Hu Z, Feng SY. Nonconventional luminescence enhanced by silicone-induced aggregation. Chem-Asian J. 2017;12:1213–7.
33. Liu B, Wang YL, Bai W, Xu JT, Xu ZK, Yang K, et al. Fluorescent linear CO_2-derived poly(hydroxyurethane) for cool white LED. J Mater Chem C. 2017;5:4892–8.
34. Zhang YW, Zhang Y. Nonconventional macromolecular luminogens with aggregation-induced emission characteristics. J Polym Sci Poly Chem. 2017;55:560–74.
35. Du Y, Yan HX, Huang W, Chai F, Niu S. Unanticipated strong blue photoluminescence from fully biobased aliphatic hyperbranched polyesters. ACS Sustain Chem Eng. 2017;5:6139–47.
36. Niu S, Yan HX, Chen Z, Li S, Xu P, Zhi X. Unanticipated bright blue fluorescence produced from novel hyperbranched polysiloxanes carrying unconjugated carbon-carbon double bonds and hydroxyl groups. Polym Chem. 2016;7:3747–55.
37. Niu S, Yan HX, Chen Z, Yuan L, Liu T, Liu C. Water-soluble blue fluorescence-emitting hyperbranched polysiloxanes simultaneously containing hydroxyl and primary amine groups. Macromol Rapid Commun. 2016;37:136–42.
38. Niu S, Yan HX, Li S, Xu P, Zhi X, Li T. Bright blue photoluminescence emitted from the novel hyperbranched polysiloxane-containing unconventional chromogens. Macromol Chem Phys. 2016;217:1185–90.
39. Zhang T, Howell BA, Dumitrascu A, Martin SJ, Smith PB. Synthesis and characterization of glycerol-adipic acid hyperbranched polyesters. Polymer. 2014;55:5065–72.
40. Asakuma Y, Maeda K, Kuramochi H, Fukui K. Theoretical study of the transesterification of triglycerides to biodiesel fuel. Fuel. 2009;88:786–91.
41. Niu S, Yan H, Chen Z, Du Y, Huang W, Bai L, et al. Hydrosoluble aliphatic tertiary amine-containing hyperbranched polysiloxanes with bright blue photoluminescence. RSC Adv. 2016;6:106742–53.
42. Li Q, Tang Y, Hu W, Li Z. Fluorescence of nonaromatic organic systems and room temperature phosphorescence of organic luminogens: the intrinsic principle and recent progress. Small. 2018;14:1801560.
43. Chen X, Luo W, Ma H, Peng Q, Yuan WZ, Zhang Y. Prevalent intrinsic emission from nonaromatic amino acids and poly(amino acids). Sci Chin Chem. 2018;61:351–9.
44. Tomalia DA, Klajnert-Maculewicz B, Johnson KAM, Brinkman HF, Janaszewska A, Hedstrand DM. Non-traditional intrinsic luminescence: inexplicable blue fluorescence observed for dendrimers, macromolecules and small molecular structures lacking traditional/conventional luminophores. Prog Polym Sci. 2019;90:35–117.
45. Niu S, Yan HX, Li S, Tang C, Chen Z, Zhi X, et al. A multifunctional silicon-containing hyperbranched epoxy: controlled synthesis, toughening bismaleimide and fluorescent properties. J Mater Chem C. 2016;4:6881–93.
46. Lu H, Zhang J, Feng S. Controllable photophysical properties and self-assembly of siloxane-poly(amidoamine) dendrimers. Phys Chem Chem Phys. 2015;17:26783–9.
47. Yan J, Zheng B, Pan D, Yang R, Xu Y, Wang L, et al. Unexpected fluorescence from polymers containing dithio/amino-succinimides. Polym Chem. 2015;6:6133–9.
48. Wang Y, Bin X, Chen, Zheng S, Zhang Y, Yuan W. Emission and emissive mechanism of nonaromatic oxygen clusters. Macromol Rapid Commun. 2018;39:1800528.
49. Li Z, Zhang L, Zhao W, Li X, Guo Y, Yu M, et al. Fluoranthene-based pyridine as fluorescent chemosensor for Fe^{3+}. Inorg Chem Common. 2011;14:1656–8.
50. Zhang S, Li J, Zeng M, Xu J, Wang X, Hu W. Polymer nanodots of graphitic carbon nitride as effective fluorescent probes for the detection of Fe^{3+} and Cu^{2+} ions. Nanoscale. 2014;6: 4157–62.